# Elastic behavior of bolted connection between cylindrical steel structure and concrete foundation

Hoang Van-Long, Jaspart Jean-Pierre, Demonceau Jean-François
ArGEnCo Department, University of Liège, Belgium

Corresponding author:
Hoang Van Long
Chemin des Chevreuils, 1 B52/3, 4000 Liège, Belgium
Phone: +3243669614
E-mail: s.hoangvanlong@ulg.ac.be

***Key words***: cylindrical structures; column base; bolted connections; elastic behaviour; component method

## Highlights

- Bolted cylindrical steel structures – concrete foundation connection is investigated
- An analytical model to obtain the elastic response of the connection is proposed
- The effect of the bolt preloading is taken into account
- The long time and volume behaviours of concrete is considered
- The calculation procedure is given with illustrative examples

***Abstract***: the paper deals with bolted connection between cylindrical steel structures and concrete foundations. In the considered connection, the circular steel structure of large diameter is welded to a base plate, and then anchor bolts are used to connect the base plate to the concrete foundation. Repartition plates are also placed to ensure an appropriate distribution of the stresses from the steel parts into the concrete. The studied configuration is often met in industrial chimneys, wind towers, cranes, etc. To characterise the studied connection, elastic model is more relevant than plastic model

but no appropriate and efficient tools for the characterisation of its elastic behaviour are available in the codes and literatures.

In the present paper, a complete analytical procedure is proposed to predict the elastic responses of the connection from their geometrical and material characteristics. Several effects are taken into account in the model, such as the effect of the bolt preloading, the long term effects in the concrete and 3D behaviour of the concrete foundation. The analytical results are validated through comparisons with numerical results. Numerical examples are also given to illustrate the proposed calculation procedure.

***Notations***

*Materials*

$E_s$ and $\nu_s$ are the Young modulus and Poisson ratio of the steel plates respectively

$E_b$ is the Young modulus of bolt material

$E_c$ and $\nu_c$ are the Young modulus and Poisson ratio of the concrete respectively

$\varphi(t)$ is the creep coefficient of the concrete at time $t$

$\delta_{shrinkage}$ is the deformation due to the shrinkage of the concrete at time $t$

*Geometrical parameters*

$a_1$ is the distance from the base plate edge to the repartition plate edge (the wall side)

$a_2$ is the distance from the base plate edge to the repartition plate edge (the free side)

$b$ is the width of the sub-part (equals to the base/repartition plate width)

$b_{eff}$ is the effective width of the base plate

$c$ is the flange width of the equivalent rigid T-stub of the repartition plate

$d$ is the nominal diameter of the bolt

$d_w$ is the diameter of the washer

$e_{01}$ is the distance from the bolt centre to the prying force position (with preload effect)

$e_{02}$ is the distance from the bolt centre to the prying force position (without preload effect)

$e_1$ is the distance from the centre of the tube wall to the bolt centre

$e_2$ is the distance from the bolt centre to the free edge of the base plate

$e_x$ is the distance from the centre of the tube wall to the base plate edge

$H_c$ is the height of the concrete part between two repartition plates

$l_b$ is the grip length of the bolt

$r_w$ is the radius of the tube wall (structure body)

$r_b$ is the radius of the bolt pitch

$t_b$ is the thickness of the base plate

$t_p$ is the thickness of the repartition plate

$t_w$ is the thickness of the tube wall

$w$ is the width of the repartition plate

$w_r$ is the width of the rigid part of the repartition plate

*Forces*

$B_0$ is the initial preload in the bolt

$B_1$ is the force in the bolt from which the preload effect is absence

$F_t$ and $F_c$ are respectively the tension and compression forces applied to the sub-part

$F_1$ is the tension force from which the preload effect is absence

$M$ is the bending moment applied to the whole connection

$M_b$ is the bending moment in the bolt shank (at the bolt head)

$M_w$ is the bending moment in the tube wall (at the section attached to the base plate)

$N$ is the axial force applying to the whole connection

*Rigidities*

$E_sI$ is the bending rigidity of the base plate (equivalent beam)

$G_sA$ is the shear rigidity of the base plate (equivalent beam)

$k_{\Delta,b}$ is the rigidity of the bolt in tension

$k_{\theta,b}$ is the rigidity of the bolt in bending

$k_{\Delta,c}$ is the rigidity of the concrete under compression

$k_{\theta,c}$ is the rigidity of the concrete under bending

$k_w$ is the flexural rigidity of the tube wall

$K_{t1}$ is the rigidity of the sub-part in tension with the preload effect

$K_{t2}$ is the rigidity of the sub-part in tension without the preload effect

$K_c$ is the rigidity of the sub-part in compression

# 1. Introduction

Normally, cylindrical steel structures with large diameters, such as industrial chimneys, wind towers, cranes, etc., are connected to a concrete foundation by a bolted joint (Fig.1). For this type of connection, the body of the structure is welded to a base plate, and then the anchor bolts are used to connect the base plate to the foundation. Repartition plates are also placed to ensure an appropriate distribution of stresses from the steel parts into the concrete foundation.

Globally, this type of structure works as a cantilever beam; therefore, the characteristics of the structure-foundation connection strongly influences the overall

behaviour of the structure. Moreover, experience shows that the base connection of the structure is the zone where premature failures often occur, mainly due to fatigue in the bolts. So the design and execution of the structure-foundation connection require an important vigilance.

Since the diameter of the assembly is very large (about 2 m to 6 m), and the bending effect is predominant in the structure body, the use of a plastic model would result in important ductility requirements that most configurations could not meet in the practice. Therefore, an elastic approach appears to be the most relevant one. In addition, an elastic model can provide useful information, as the connection rigidity, the evolution of the stress in the elements. These information allow to assess the fatigue strength or calculate static/dynamic responses of the structure in the design process.

Concerning the design codes, the following remarks can be drawn: EN-1993-1-8 (design of joints) [8] provides rules for calculating column bases, especially for columns in buildings with I / H sections. So, improvements of these rules is required in order to cover the joint configuration investigated here. EN-1993-1-9 dedicated to fatigue design [9] provides us details to estimate the fatigue resistance of elements of steel structures. The bolt is classified as a nominal detail for which the effects of bending and prying must be considered. However, the determination of the stress in the bolt taking into account these effects in the elastic range is questionable in many cases. Other codes may be considered, such as CEN/TS1992-4-1 (Design of fastenings) [7], EN1993-3-1 and 3-2 (Design of towers, mats and chimneys) [10, 11]

or EN1993-4-1 (Design of Silos) [12] but they do not specifically address the design of connections between cylindrical structures and concrete foundations.

Looking in literature, several researches regarding the behaviour of column bases [e.g. 13, 14, 16, 17, 19, 20, 21, among others] have been carried out in the past 20 years. Most of them investigate the possibility to extend the component method (initially developed for beam-to-column) to column bases of buildings with columns with I, H or hollow sections. The application of these results on the analysis of cylindrical structures, especially in the elastic range, require more developments. In particular, the presence of bolt preloading is not addressed in the existing tools, due to a lack of knowledge in terms of loss of preload in the anchor bolt.

Due to the above mentioned reasons, engineers encounter difficulties when designing the considered type of assembly and sophisticated numerical model through finite element methods is often used, even it is known to be expensive and time consuming.

In the present paper, a complete analytical procedure is proposed to predict the elastic responses of the connection from their geometrical and material characteristics. Several effects are taken into account in the model, such as the effect of the bolt preloading, the long term effects in the concrete and 3D behaviour of the concrete foundation. The analytical results are validated through comparisons to numerical results. Numerical examples are also given to illustrate the proposed calculation procedure.

## 2. Behaviour of a sub-part of the connection

As the considered connection is axis-symmetric (both geometry and material), the studies may be carried out on a sub-part, as described in Fig.2; this is a *1/n* part with *n*, the number of anchor bolts. By extracting this sub-part from the circular connection,

this means that the shape of the plates is quite complex. However, for sake of simplicity, a rectangular form is adopted for the conducted investigations. As the diameter of the connection and the number of bolts are normally significant, the above assumption leads to negligible uncertainties. The width, *b*, of the sub-part may be estimated as the arc length at the level of the bolts (place on a circle with a radius $r_b$ – see Fig.2 ), meaning that *b* may be calculated by Eq.(1).

$$b = \frac{2\pi r_b}{n} \tag{1}$$

When the whole structure is subjected to external loads (i.e. horizontal and vertical loads), the tension/compression forces are transferred to the sub-part through the structure wall. Accordingly, based on the component method concept, the following components should be considered to obtain the behaviour of the sub-part:

- Structure wall in traction/compression and bending
- Base plate in flexion and shear
- Bolt in tension and bending
- Repartition plate in bending
- Concrete in compression

The mentioned components will be characterized in Section 2.1. The procedure to obtain the global behaviour of the sub-part will be presented in Section 2.2. Then, the asseembly procedure of the sub-part to obtain the whole joint behaviour will be dealt with in Section 3. The calculation procedure will be summarized in Section 4. Section 5 aims at validating the proposed method and at illustrating the calculation procedure. Section 6 finally addresses some conclusions.

## 2.1. Behaviour of individual components

### *2.1.1. Structure wall component*

The structure wall plays two roles (Fig.3): (1) transfer the tension/compression force from the structure body to the base plate; and (2) restrain the rotation of the base plate. Within the proposed model, the second role is considered by simulating the restraining effect through an elastic rotational spring with an appropriate rigidity $k_w$. To determine $k_w$, the structure body is modelled by a cylindrical shell with an infinitive length; the centripetal displacement at the end of the cylindrical shell is blocked by the base place. $k_w$ is defined as the ratio between the applied moment and the rotation at the end of the shell wall. Through classical mechanical approaches, it is easy to deduce the following equation for $k_w$ (details of the intermediate quantities may be found in [18]):

$$k_w = 2\beta D b \tag{2}$$

with $D = \frac{E_s t_w^3}{12\left(1-\nu_s^2\right)}$, the bending rigidity of the shell and $\beta = \sqrt[4]{\frac{E_s t_w}{4 r_w^2 D}}$ where $E_s$ and $\nu_s$ are respectively the Young modulus and the Poisson coefficient of the steel tube, $r_w$ and $t_w$ are the radius and the thickness of the steel tube and b is the width of the sub-part.

### *2.1.2. Base plate component*

The behaviour of the base plate is similar to the flange of a standard T-stub as defined in the component method [8]. Therefore, the base plate may be modelled by an equivalent beam with a section width equals to 0.85*b* (Fig.4), as recommended in [14] for T-stub in the elastic range:

$$b_{eff} = 0.85b \quad (3)$$

*2.1.3. Anchor bolt component*

In the present work, the two following specificities are recommended for the anchor bolts:

(1) In many cases, a nut is placed under the repartition plate to facilitate the build-up procedure; however, with the presence of this nut, most of the bolt length is not preloaded (Fig.5), meaning that the fatigue resistance is considerably reduced (the fatigue often occurs just under the mentioned nut). So, it is recommended here to place no nut under the repartition plate.

(2) A direct contact between the bolt and the concrete results in a concentration of stresses in the bolt shank (Fig.6), reducing also the fatigue resistance of the bolts. So, it is recommended here to avoid such contact by placing, for instance, plastic tubes around the bolts shank before the concrete casting procedure may be used.

Considering the two above mentioned specificities, the bolt may be modelled as a clamped-pinned bar, as seen in Fig.7. The length ($l_b$) of the bar is considered as equal to the distance between the lower face of the lower reparation plate and the upper face of the base plate (Fig.7); this corresponds to the grip length of the bolt. By using this model, the rigidities in tension and flexion of the bolt can be formulated. As the tension force in the bolt is important, it is recommended to take into account the effect of the tension force on the rigidity in flexion by using the stability functions. Accordingly, the rigidity in tension rigidity ($k_{\Delta,b}$) and the rotational rigidity ($k_{\theta,b}$) can be respectively determined through Eq.(4) and Eq.(5):

$$k_{\Delta,b} = \frac{E_b A_b}{l_b} \tag{4}$$

$$k_{\theta,b} = \frac{E_b I_b}{l_b} S \tag{5}$$

In Eqs.(4) and (5), $E_b$ is the Young modulus of the bolt material; $l_b$ is the bolt length (Fig.7); $A_b$ and $I_b$ are the area and the second moment of the cross-section of the bolt respectively(of the threated or non-threated portion according to the bolt configuration). $S$ is the stability function that can be found in many references (e.g [2]):

$$S = \frac{(kl_b)^2 \cosh(kl_b) - kl_b \sinh(kl_b)}{2 - 2\cosh(kl_b) + kl_b \sinh(kl_b)} \tag{6}$$

with $k = \sqrt{B / E_b I_b}$ where $B$ is the force in the bolt, and $E_b I_b$ is the flexion modulus of the bolt. In fact, $B$ varies according to time (due to loss of preloading and due to external load); for the sake of simplification, the initial value $B_0$ may be adopted, $B_0$ being equal to the initial preloading subtracting the loss associated to the creep and shrinkage of the concrete. The details on the loss part will be dealt with in Section 2.1.6. For practical purpose, some concrete values of the stability function are given in Table 1.

*2.1.4. Repartition plate component*

In the calculation of the column bases, the flexible plate in contact with the concrete is normally replaced by a rigid plate. In this work, a model based on the equivalent rigid plate proposed in [16] is applied, in which equivalence condition on the displacement between the flexible and rigid plates (Fig.8) is adopted, and the rigid plate dimension are defined through the definition of the parameter $c$ (Fig.8):

$$c = 0,66\sqrt[3]{\frac{E_s}{E_c}}t_p \tag{7}$$

In Eq.(7), $E_s$ and $E_c$ are the Young modulus of the repartition plate and of the concrete respectively; $t_p$ is the thickness of the repartition plate. In the case where $E_s$=210000 N/mm$^2$ and $E_c$=300000 N/mm$^2$ , one has $c = 1.25t_p$ .

With the present case, two situations can be identified, depending on the considered contact zone between the base plate and the repartition plate:

(1) A punctual contact for which the contact zone is simplified as a line (Figs. 9a and 9b); this situation is met in the case of a free contact between the plate and the repartition plate.

(2) A contact zone spreading on a certain area (Figs. 9c and 9d) in situation where the contact between the two plates is imposed by the bolt. The nut (or bolt head) is considered as rigid and a 45 degree diffusion is assumed in the base plates.

From the above assumptions and the actual geometries of the plates, the dimension of the rigid part of the repartition plate can be obtained (Table 2).

*2.1.5. Concrete block component*

In EN-1993, part 1.8 [8], the rigidity of the concrete block is given by:

$$k_{c,EN} = \frac{E_c\sqrt{b_{eff\_EN}l_{eff\_EN}}}{1.275}$$

with $E_c$, the concrete Young modulus; $b_{\text{eff\_EN}}$ and $l_{\text{eff\_EN}}$, respectively the width and the length of the effective part of the repartition plate (or base plate if a repartition plate is not placed).

The following assumption have been used in EN-1993, part 1.8 [8] to deduct the above expression for the rigidity of the concrete:

- A coefficient of 1.5 is used to reduce the rigidity in order to consider the poor quality of the concrete surface in contact with the plate.
- The concrete block is considered as a half elastic space, a coefficient with a fixed value of 0.85 is used to take into account the dimensions ($b_{\text{eff\_EN}}$ and $l_{\text{eff\_EN}}$) of the effective plate (rigid plate). This means that the different dimensions of the plate are disregarded.

For the present case, it is proposed that:

- The quality of the concrete at the surface between the concrete and the repartition plate is supposed to be “perfect”, meaning the reduction on the rigidity is not required (i.e. the reduction coefficient equals to 1.0). This assumption is based on the fact that the repartition plate is directly embedded in the concrete; this plate is placed before the concrete casting.
- The volume effect should be considered for each case, depending on the dimensions of the rigid plate and the concrete block. This consideration is performed as explained here after.

As a sub-part is extracted from the whole connection (Fig.2), the lateral deformation of the sub-part is locked; a plane deformation behavior may be adopted, meaning that the 3D problem becomes a 2D problem. Moreover, it is assumed that only the deformation of the concrete part above the lower repartition

plate is considered ($H_c$ in Fig.10). The actual width ($L_c$) of the concrete, symmetric with respect to the rigid plate (Fig.10), is taken into account in the model.

The rigidity of the concrete block may be obtained through the expression (8):

$$k_{\Delta,c} = \frac{E_c}{\alpha_\Delta} b \tag{8}$$

with $E_c$, the concrete Young modulus; $b$, the width of the sub-part (Eq.(1)); $\alpha_\Delta$, a coefficient taking into account of the volume effect, depending on relative dimensions between the plate ($w_R$) and the concrete block ($H_c$ and $L_c$): $\alpha_\Delta = f\left(H_c / w_R, L_c / w_R\right)$. In the present work, this coefficient $\alpha_\Delta$ is numerically determined. A plane deformation problem was introduced assuming an elastic material behavior for the concrete and a "rigid" material behavior for the rigid plate. A concentrated load (F) is applied at the center of the plate (Fig. 10). With such values of $H_c/w_R$ and $L_c/w_R$, we can numerically obtain a displacement $\delta$ from which the coefficient $\alpha_\Delta$ can be determined using the following equation:

$$\alpha_\Delta = \frac{E_c \delta b}{F}$$

This equation is deduced from Eq.(8) by setting $k_{\Delta,c} = F/\delta$ (as the definition of the rigidity).

By varying $H_c/w_R$ and $L_c/w_R$, different values of $\alpha_\Delta$ can be obtained. Values covering practical configurations are given in Table 3; the corresponding graphic is given in Fig.11.

*Rotational stiffness*

Formula (8) is established for the case where the force is applied at the center of the plate. When a bending moment is added (associated to an eccentric load), the

plate exhibits rotation displacement in addition to the vertical displacement. The eccentricity of the load is often associated to the eccentricity in the load transfer from the base plate (in bending) to the repartition plate through the bolts (Fig. 9c and 9d). Therefore, the rigidity of the system may be modelled by two springs, one translational ($k_{\Delta,c}$) and one rotational ($k_{\theta,c,}$ see Fig. 12). The translational spring rigidity ($k_{\Delta,c}$) is given by Eq.(8) while the rotational spring rigidity may be determined by the following equation:

$$k_{\theta,c} = \frac{E_c w_R^2 b}{\alpha_\theta} \tag{9}$$

with $E_c$, the Young modulus of concrete, $w_R$, the width of the rigid plate, $b$, the width of the sub-part, $\alpha_\theta$, a coefficient defined here after. Eq.(9) is based on the assumption that a full contact between the plate and the concrete is ensured; this assumption is acceptable as the concrete under the rigid part is normally in compression on all its area. Physically, the $w_R^2 b$ term in Eq.(9) represents the flexion modulus of the rigid plate. Again, $\alpha_\theta$ is determined numerically through the same method used to determine $\alpha_\Delta$ (Eq.(8)); only the compression force is replaced by a bending moment (Fig. 12). From the numerical results, it is observed that the influence of the $H_c/w_r$ ratio is not significant; so this parameter is taken out. Table 4 gives the values of the coefficient $\alpha_\theta$ which can be used to determine the rigidity of the plate through (Eq.(9)).

*2.1.6. Loss of preloading in the bolt*

In such joint configuration, a loss of preloading in the bolts may be observed due to the fact that the concrete properties are time-dependent, and also due to the

relaxation of the bolts. In the present work, the loss of preloading caused by creep and shrinkage of the concrete is considered while the relaxation of the bolts is neglected as it is generally not significant.

The creep phenomenon may be represented by a diminution of the concrete stiffness according to the time. Using EN-1992, part 1.1 [6] the concrete Young modulus, $E_c(t)$, at the time $t$, can be estimated taking into account the creep effect, from the initial Young modulus ($E_c(0)$): $E_c(t) = E_c(0)\varphi(t)$ where $\varphi(t)$ is the creep coefficient. As the rigidity of the concrete block (Eq.(8)) is directly proportional to the Young modulus $E_c$ , therefore we can write: $k_{\Delta,c}(t) = \varphi(t)k_c(0)$.

Let us consider a system of concrete and anchor bolt (Fig. 13) at three different steps: before preloading, just after preloading and at a moment $t$. At the initial stat (i.e. before preloading – see Fig. 13), there is no stress in the concrete and the bolt; the length of the concrete is bigger than the one of the bolt. Just after preloading, the compression force in the concrete is in equilibrium with the tension force in the bolt ($B(0)$), and the length of the concrete block is equal to the length of the bolt. At time $t$, due to the decrease of the concrete rigidity, the length of the system decreases; the compression force in the concrete is still in equilibrium with the tension force in the bolt but the value is reduced ($B(t)$). It is easy to obtain the reduction $\Delta B$ to pass from $B(0)$ to $B(t)$ through the following equation:

$$\Delta B_{creep}(t) = B_0 \left( 1 - \frac{1 + \frac{k_{\Delta,b}}{k_{\Delta,c}(0)}}{1 + \frac{k_{\Delta,b}}{\varphi(t) k_{\Delta,c}(0)}} \right) \tag{10}$$

where $k_{\Delta,b}$ is the axial rigidity of the bolt given by Eq.(4) while $k_{c,0}$ is the initial rigidity of the concrete given by Eq.(8).

Eq.(10) points out that the loss of the preloading due to creep is proportional to the $k_b/k_{c,0}$ ratio; this remark is useful as it will allow to select an appropriate length and diameter for the bolt in order to limit the loss of preloading in a reasonable way.

With respect to the shrinkage effect, the deformation of the concrete due to this phenomenon can be also determined using EN-1992, part 1.1 [6]: $\delta_{\text{shrinkage}}(t) = \varepsilon_{\text{shrinkage}}(t) L_c$ where $\varepsilon_{\text{shrinkage}}(t)$ is the shrinkage deformation at time $t$. Therefore, the loss of the preloading at time $t$ caused by the shrinkage may be calculated by:

$$\Delta B_{shrinkage}(t) = k_{\Delta,b}\delta_{shrinkage}(t) \tag{11}$$

From Eq.(10) and Eq.(11), one obtains the total loss of preload caused by both creep and shrinkage:

$$\Delta B(t) = B_0\left(1 - \frac{1+\dfrac{k_{\Delta,b}}{k_{\Delta,c}(0)}}{1+\dfrac{k_{\Delta,b}}{\varphi(t)k_{\Delta,c}(0)}}\right) + k_{\Delta,b}\delta_{shrinkage}(t) \tag{12}$$

From Eq.(12), it can be observed that the two key quantities affecting the loss of preloading in the bolt are $\varphi(t)$ and $\delta_{\text{shrinkage}}(t)$. The method to determine these parameters is available in EN-1992, part 1.1 [6]; they are not given herein. In references [3] and [4], the procedure to estimate the loss of preloading in anchor bolts are also presented; however, it seems that the rigidity of the concrete block is determined from the experimental results, not by the analytical one.

### 2.2. Assembling procedure

In this section, how to obtain the elastic response of the sub-part from the rigidities of the individual components given in Section 2.1 is explained. In particular, two quantities will be determined: the global rigidity of the sub-part and the internal forces in the bolt (axial force and bending moment). The reasons are that: the rigidity of the sub-part is required to distribute the loads within the global connection subjected to moment and axial forces and, the internal forces in the bolts (and in particular the associated stresses) are required to assess the fatigue behaviour, which regularly leads to the failure of the bolts if not well assess. The other quantities such as stress in the base plate or in the tube wall can be easy obtained from the defined ones.

### *2.2.1. Preliminary information*

The following points have to be clarified before assembling the components.

*Preloading effect on the concrete + bolts component*

Concrete and bolt work together when the preloading effect is still active and they work separately when the preloading effect is absence (Fig. 14). Therefore, under the tension force at the base plate, the rigidity of the concrete + the bolt is equal to the sum of the individual rigidities of the concrete and of the bolt ($k_{\Delta,b} + k_{\Delta,c}$) when the preloading is still present; but the rigidity is equal to the one of the bolt only ($k_{\Delta,b}$) if the preloading is not present.

*Position of the prying force between the base plate and the repartition plate*

It is clear that with the bolt preloading, the position of the prying force moves from the bolt centre to the plate edges, depending on the evolution of the applied force. For the sake of simplification, only two situations are considered in the calculation: (1) the farthest position of the prying force when the preloading is present; and (2) the farthest position of the prying force when the preloading is not present.

For the first position, the distance between the bolt and the prying force is approximated as (Fig. 15):

$$e_{01} = \min(2e_2/3, \quad 0.5d + 0.74t_p) \tag{13}$$

with $e_2$, the distance between the bolt centre and the base plate edge; $d$, the bolt diameter; and $t_p$, the thickness of the base plate. In Eq.(13), "$2e_2/3$" and "$0.74t_p$" terms are proposed in [1], in this work "$0.5d$" is added to take into account of the bolt dimension.

In the case without the preloading, the position of the prying force in a T-stub as defined in EN-1993, part 1.8 [8] may be applied for the present case (Fig. 15):

$$e_{02} = \min(e_2, \quad 1.25e_1) \tag{14}$$

*Limit point for which the preloading has to be considered or not*

As mentioned previously, under the tension load, the sub-part is analysed for two distinguished situations: with or without bolt preloading. In each case, the evolution of the internal force in the bolt according to the applied external force can be determined. The increase of the force in the bolt in the "no preloading" situation is more important than in the "preloading" situation as illustrated in Fig.16. The intersection point between the two lines, (($B_1$, $F_1$) point in Fig. 16), is assumed as the limit to pass from one situation to another. The detailed values of $B_1$ and $F_1$ will be provided for different cases in Section 2.2.2. The continuous broken line in Fig.16 represents the considered evolution of the internal force in the bolt.

*Sub-part in compression*

It is assumed that the rigidity of the sub-parts in compression is constant and that the preloading is still always present.

### *2.2.2. Assembly formulation*

From the individual component rigidities given in Section 2.1 and the remarks reported in Section 2.2.1, the assembly procedure can be defined and carried out. The results are presented in Tables 5, 6 and 7. In these tables, the mechanical models are firstly reported and then the formulas that are obtained by analysing the mechanical models are given. The mechanical models have a level 2 of hyper-staticity, so they can be easily solved through analytical approaches, as the force method or the displacement method.

Beside the quantities detailed in Table 5, 6 and 7, other quantities (as forces in the tube wall or forces in the base plate) can be easily predicted using equilibrium equations.

## 3. Global connection characterisation

This section aims at providing the procedure to estimate the global behaviour of the connection. The main objective is to obtain, according to the applied moment ($M$) and axial force ($N$) on the connection:, (1) the global rigidity of the connection; and (2) the force distribution in each sub-part in tension and compression (from which the elastic responses of the sub-part may be accordingly deduced) .

The behaviour of the connection under a bending moment and a compression force is described in Fig. 17. For the sake of simplification, the cross-section of the structures wall is supposed to remain plane during the loading, therefor the kinematic of the connection can be controlled by two parameters: position of the neutral axis (given by the angle $\alpha$ in Fig. 17a), and the rotation (represented by $\theta$ in Fig. 17a). The following principles are followed to analyse the system:

- The displacement at any point of the connection are written as functions of the angle $\alpha$ and the rotation $\theta$.
- With the obtained displacement, using the force-displacement relationship (Fig.17b) one can determine the force in the corresponding sub-part. Meaning that these forces are also functions of $\alpha$ and $\theta$.
- From two equilibrium equations (axial force and bending moment), $\alpha$ and $\theta$ can be determined, meaning that all the previously mentioned quantities can be obtained.

In fact, the expressions become rapidly complicated; so it is not easy to manually solve the obtained equations. However, it has to be noticed that the behaviour of the connection can be numerically obtained using quite simple models once the behaviour of the sub-part is known (Fig.17b). In the numerical model, the sub-parts can be modelled through 1D "links" with a behaviour law as given in Fig. 17b while the structure wall may be replaced by "rigid" elements (1D elements can be used).

In this section, the results given in [1] are summarized, the solutions are only valid in "State A" (Fig.17), i.e. when the preloading effect is still present in the tension zone.

The angle $\alpha$ can be determined from Eq.(15):

$$\frac{M}{Nr_w} = -\cos\alpha + \frac{\sin\alpha^2\left[\alpha + K_{t1}/K_c(\pi-\alpha)\right]}{\sin\alpha - \alpha\cos\alpha - K_{t1}/K_c(\sin\alpha + (\pi-\alpha)\cos\alpha)} \tag{15}$$

In [1] a chart is provide to practically obtain the angle $\alpha$.

The rotation of the whole connection may be obtained from Eq.(16):

$$\theta_j = \frac{M_j b}{r_w^3 \left[ (K_{t1} - K_c)\left( \frac{\sin 2\alpha}{2} - \alpha \right) + \pi K_t \right]} \tag{16}$$

The tension and compression forces (in the most loaded sub-part) are:

$$\begin{aligned} F_t &= K_{t1} r_w (1 + \cos\alpha)\theta_j \\ F_c &= K_c r_w (1 - \cos\alpha)\theta_j \end{aligned} \tag{17}$$

Finally, the rigidity of the connection is calculated by:

$$S_j = r_w^3 \left[ (K_{t1} - K_c)\left( \frac{\sin 2\alpha}{2} - \alpha \right) + \pi K_{t1} \right] / b \tag{18}$$

## 4. Calculation procedure

For a given connection (geometries and materials) under *M* and *N*, the connection may be analysed using the following procedure to obtain its main properties, as its rigidity, and the stresses in the bolt.

***Step 1***: preparation of the data related to the geometry and the materials of the connection

***Step 2***: Calculation of the rigidities of the individual components

- Rotational rigidity of the structure wall ($k_w$): Eq.(2)
- Bending rigidity of the base plate ($E_s I$ and $G_s A$) and geometry of the base plate (mainly its effective width determined using Eq.(3))
- The axial and rotational rigidities of the bolt: Eqs.(4) and (5).
- The equivalent rigid part of the repartition plate: Table 2.
- Translational and rotational rigidities of the concrete block $k_{\Delta,c}$ and $k_{\theta,c}$: Eqs.(8) and (9).
- Loss of preloading in the bolt if required: Eq.(12).

***Step 3***: Calculation of the rigidity in tension and compression of the sub-part

- Rigidity in tension: Table 5 for $K_{t1}$ and Table 6 for $K_{t2}$.
- Rigidity in compression, $K_c$: Table 7.

***Step 4***: Rigidity of the connection, distribution of the force in the sub-part, force in the bolts

- Rigidity of the connection, $S_j$: Eq.(18)
- Force in the sub-part, $F_t$ and $F_c$: Eq.(17)
- Force/or stresses in bolt: Tables 5 and 6.

Some numerical examples to illustrate the above calculation procedure will be presented in the next section (Section 5).

## 5. Numerical examples and validation

This section aims at (1) validating the developed models for the sub-part behaviour proposed in Section 2 through numerical results, and (2) illustrating the design procedure given in Section 4 (Step 1 to Step 3). In total, six examples are considered, named Ex 1.1, Ex 1.2, Ex 1.3, Ex 2.1, Ex 2.2 and Ex.3; their geometries are shown in Fig.18. The same geometries are used for Exs 1.1, 1.2 and 1.3, only the bolt preloading is different. Also, the same geometries are adopted for Exs 2.1 and 2.2, but the materials are different. In the numerical models, the actual form of the sub-part, cut from a cylindrical connection (with $r_b$ = 935 mm and $r_w$ = 1042.5 mm), is introduced for Exs 1.1, 1.2 and 1.3, while the rectangular shape is adopted for Exs 2.1, 2.2 and Ex.3. M52, M30 and M36 bolts are indicated in Fig.18 but diameters of 46.5 mm, 27.0

mm and 32.0 mm are respectively used in the calculations, to take into account of the threaded portions of the bolt shanks.

The numerical analyses were carried out using LAGAMINE – a non-linear finite element programme developed at the University of Liège [15]. Elastic materials with the properties given in Table 8 are introduced; the contacts between the bolt and the base plate and between the base plate and the repartition plate are also modelled. Fig. 19 shows a general view of the mesh.

In parallel, the proposed analytical procedure is applied for the considered examples. In Table 8, not only the input data and the main results are reported but also the way they have been derived in order to illustrate the calculation procedure. Due to the space limitation, the detail of Ex.3 are not mentioned in Table 8.

The comparison of the rigidities of the sub-parts and the evolution of the forces in the bolts are presented in Figs. 20 and 21. A good agreement between the numerical and analytical analyses is observed, in particular for the rigidities under compression. With respect to the evolution of the forces in the bolts, the analytical method gives conservative values.

## 6. Conclusion

A complete analytical model devoted to the characterisation of the elastic behaviour of bolted connections between cylindrical steel structure and concrete foundation has been developed. All the required characteristics of the connection (stiffness, stress, etc.) can be obtained knowning its geometry, the constitutive materials and the applied external loads. In the proposed model, several parameters have been taken into account such as the effect of the preloading in the bolts, the bending moment in the bolt with

account of the second order effect, the time-dependent properties of the concrete block, the flexibility characteristics of the base plate and of the repartition plate, etc. The proposed model is in full agreement with the principle of the component method; therefore, the proposed model could be easily extended to other types of connections. The results of the analytical model have been compared with the ones of numerical models and a good agreement has been observed.

## Acknowledgements

This work was carried out with a financial grant from the Research Fund for Coal and Steel of the European Community, within FRAMEUP project "Optimization of frames for effective assembling", Grant $N^0$ RFSR-CT-2011-00035.

## References

[1] Couchaux M. *Comportement des assemblages par brides circulaires boulonnés* (in French) PhD thesis, INSA of Rennes, France, 2010.

[2] Chen W. F., Lui E. M. *Stability design of steel structures*. CRC Press, 1991.

[3] Delhomme F., Debicki G., Chaib Z. *Experimental behaviour of anchor bolts under pullout and relaxation tests.* Construction and Building Materials, 24(2010), pp 266-274.

[4] Delhomme F., Debicki G. *Numerical modelling of anchor bolts under pullout and relaxation tests.* Construction and Building Materials, 24 (2010), pp1232–1238.

[5] EN1090-2. *Execution of steel structures and aluminium structures - Part 2: Technical requirements for steel structures*. CEN, Brussels, 2008.

[6] EN1992-1-1: *Design of concrete structures - Part 1-1: General rules and rules for buildings.* CEN, Brussels, 2005.

[7] EN/TS1992-4-1: *Design of fastenings for use in concrete - Part 4-1: General*. CEN, Brussels, 2009.

[8] EN1993-1-8: *Design of steel structures -Part 1.8: Design of joints.* CEN, Brussels, 2005.

[9] EN1993-1-9: *Design of steel structures - Part 1.9: Fatigue*. CEN, Brussels, 2005.

[10] EN1993-3-1: *Design of steel structures - Part 3-1: Towers, masts and chimneys - Towers and masts*. CEN, Brussels, 2006.

[11] EN1993-3-2: *Design of steel structures - Part 3-2: Towers, masts and chimneys – Chimneys*. CEN, Brussels, 2006.

[12] EN1993-4-1: *Design of steel structures - Part 4-1: Silos*. CEN, Brussels, 2006.

[13] Guisse S, Vandegans D, Jaspart JP. *Application of the component method to column bases – experimentation and development of a mechanical model for characterization*. Research Centre of the Belgian Metalworking Industry, 1996.

[14] Jaspart J.P. *Recent advances in the field of steel joints – Column bases and further configurations for beam-to-column joints and beam splices*. Agregation Thesis, University of Liège, 1997.

[15] LAGAMINE - *User's manual*, University of Liege, 2010.

[16] Steenhuis M., Wald F., Stark J. *Resistance and stiffness of concrete in compression and base plate in bending*. In "Semi-rigid connections in structural steelwork", Springer Wien New-York, 2000.

[17] Steenhuis M., Wald F., Sokol Z., Stark J. *Concrete in compression and base plate in bending*. HERON, Vol. 53 (2008), $N^0$ 1/2.

[18] Timoshenko S., Woinowsky-Krieger S. *Theory of Plates and Shells*. McGraw-Hill, 1959.

[19] Wald F., Bouguin V., Sokol Z., Muzeau J.P. *Effective length of T-Stub of RHS column base plates*. Czech Technical University, 2000.

[20] Wald F., Sokol Z, Jaspart J.P. *Base plate in bending and anchor bolts in tension*. HERON, Vol. 53 (2008), $N^0$ 2/3.

[21] Wald F., Sokol Z, Steenhuis M., Jaspart J.P. *Component method for steel column bases*. HERON, Vol. 53 (2008), N0 2/3.

## List of Figures

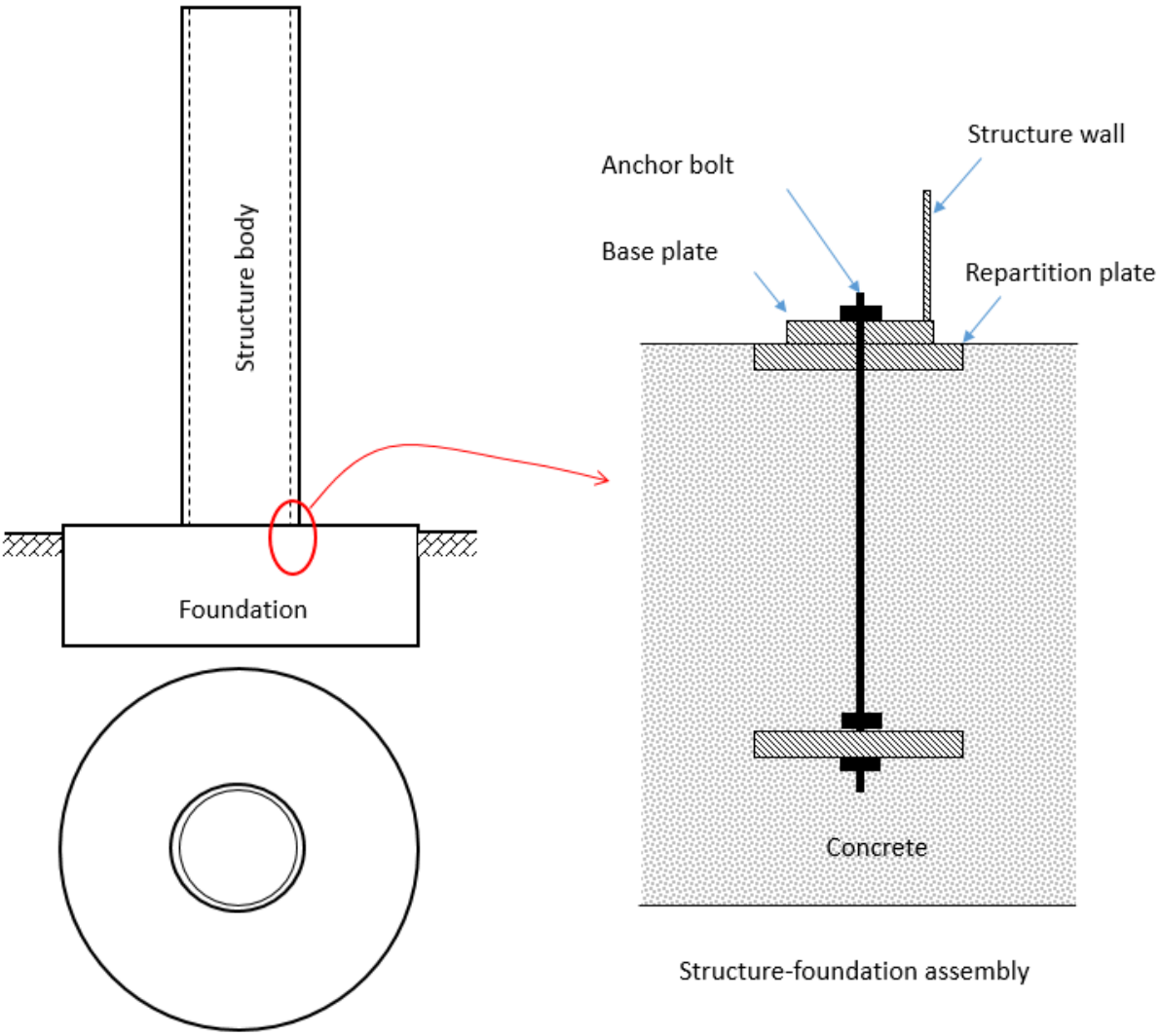


Fig.1. Considered connection

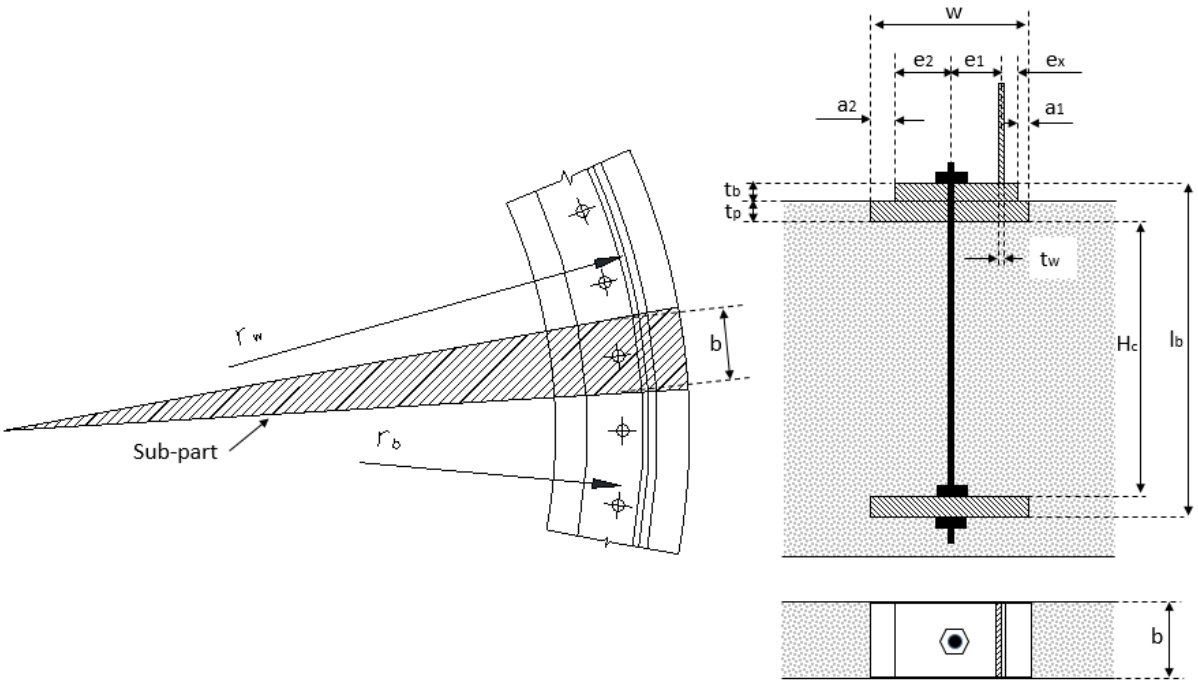


Fig.2. Geometries of the sub-part

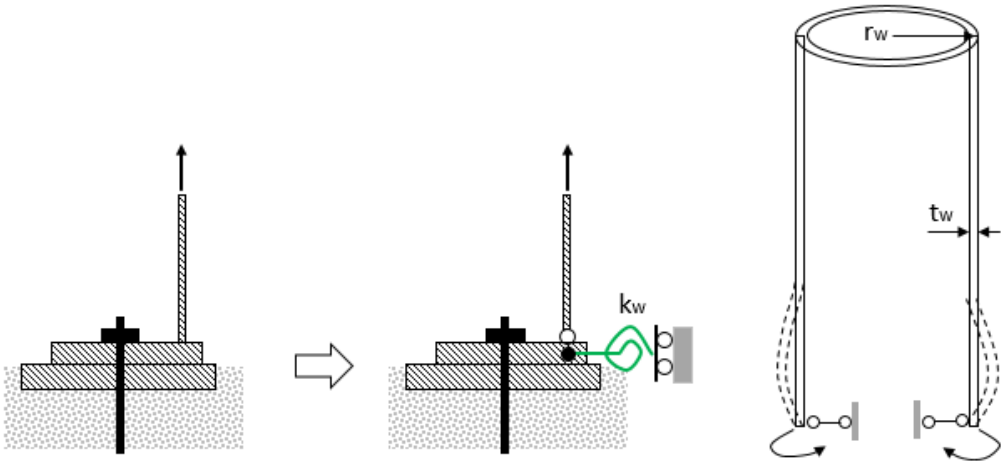


Fig.3. Rotational rigidity of the tube wall

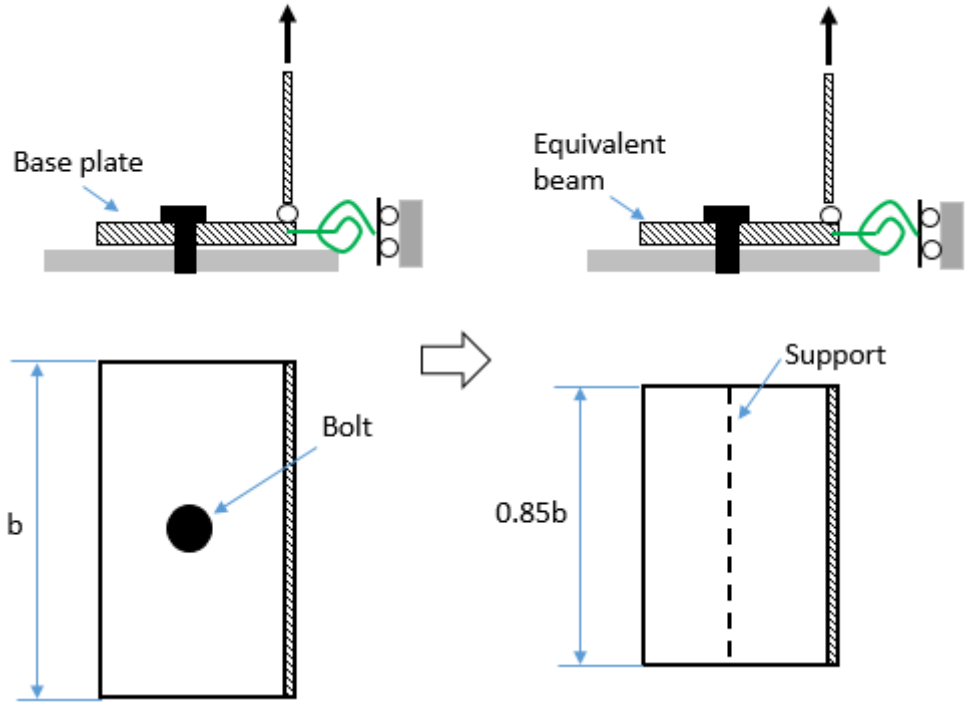


Fig.4. Effective width of the base plate

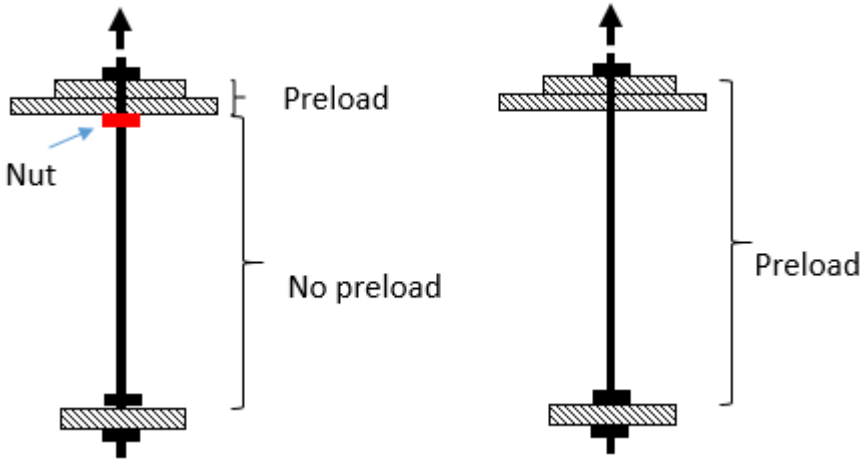


Fig.5. Effect the nut under the repartition plate

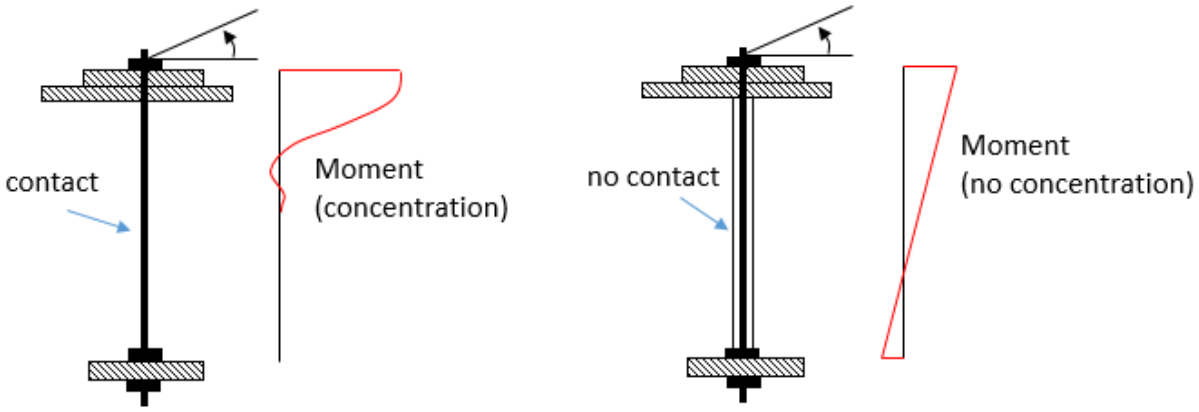


Fig.6. Effect of the direct contact between the bolt and concrete

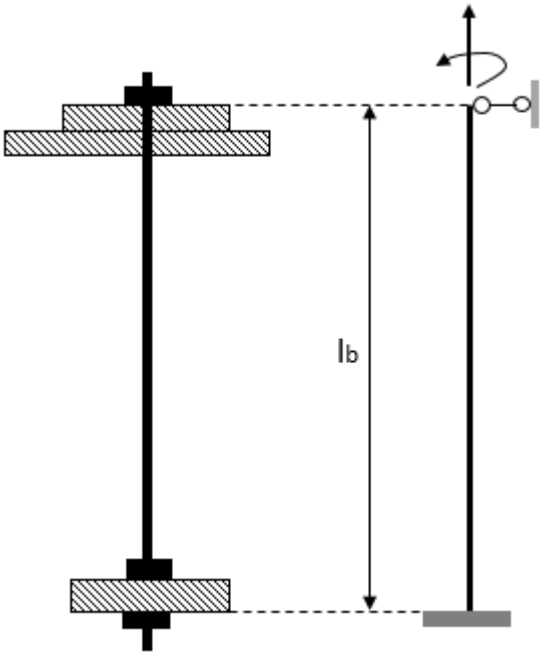


Fig.7. Bolt modelling

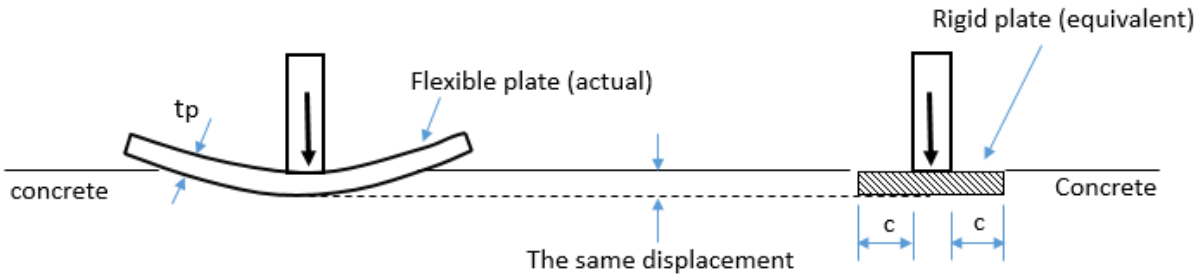


Fig.8. Equivalent part of the repartition plate

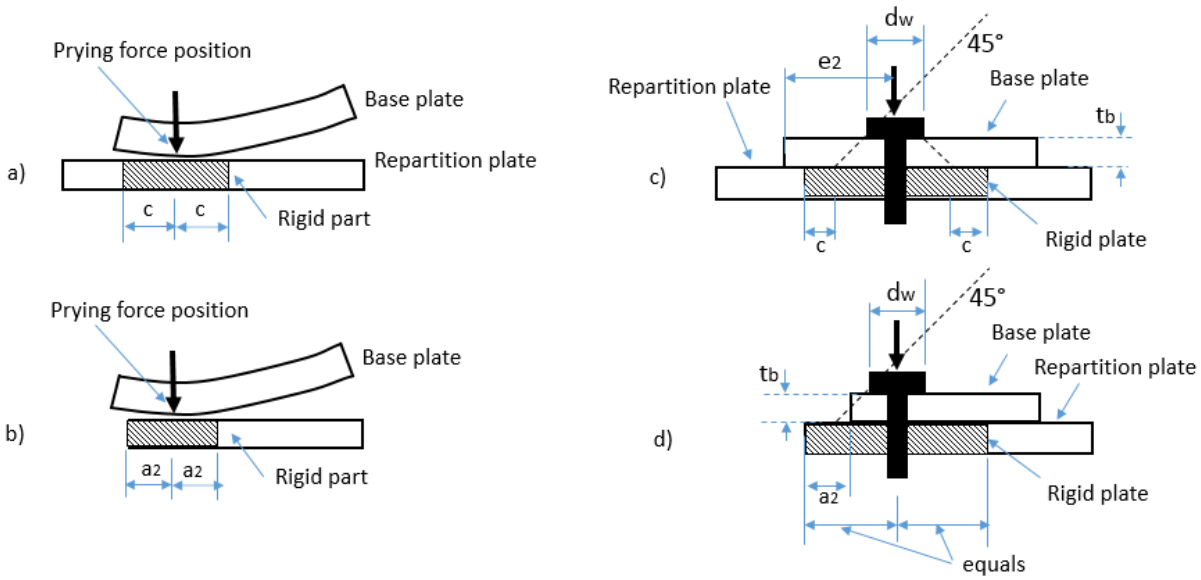


Fig.9. Determination of rigid part ($w_r$) of the repartition plate

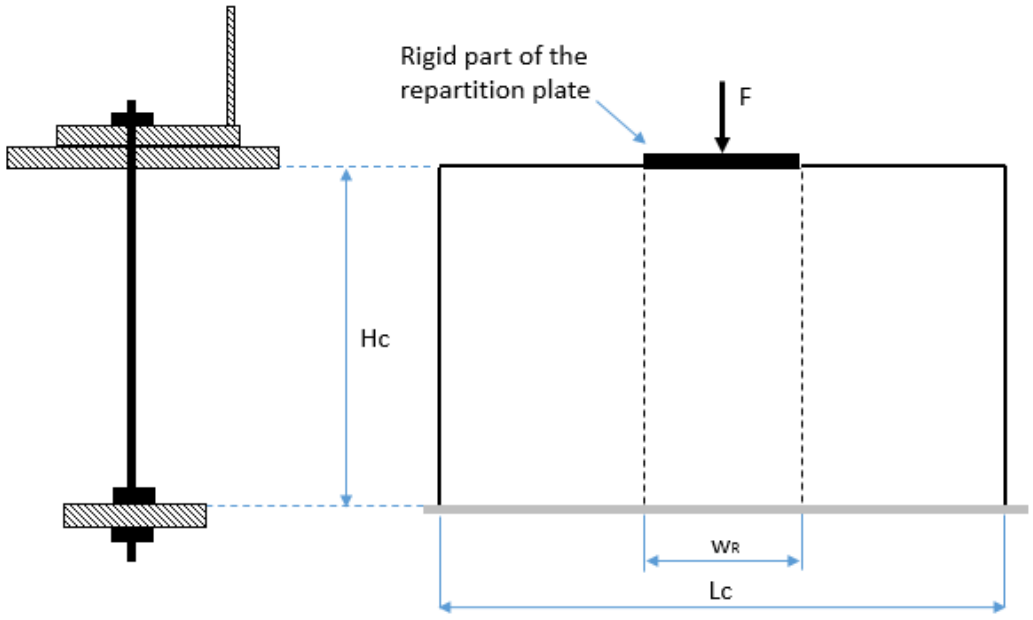


Fig.10. Considered size of the concrete block

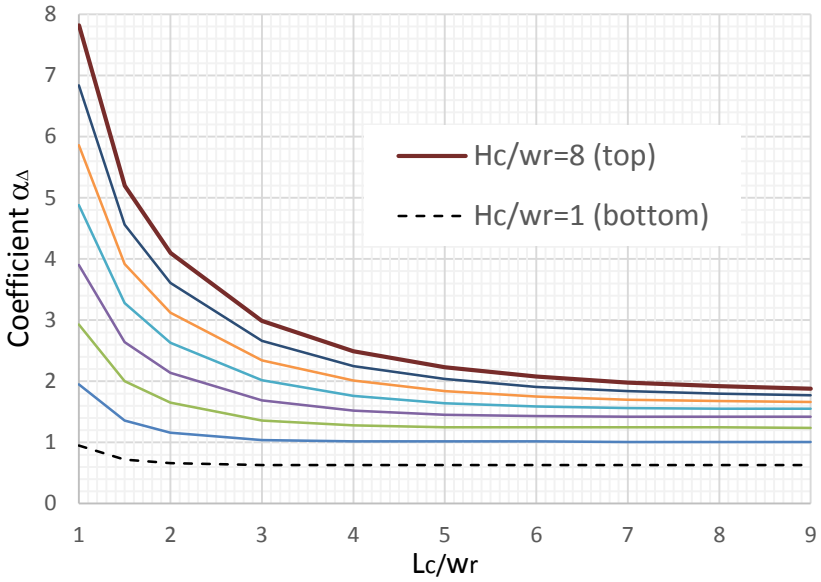


Fig.11. Evolution of $\alpha_\Delta$ according to $H_c/w_r$ and $L_c/w_r$

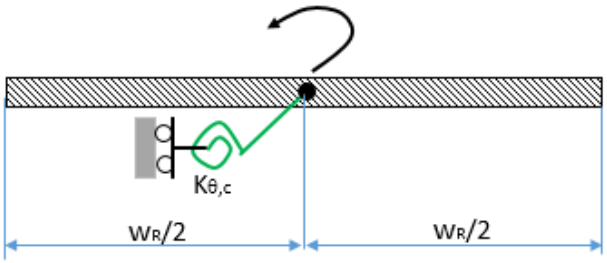


Fig.12. Rotational rigidity of the concrete

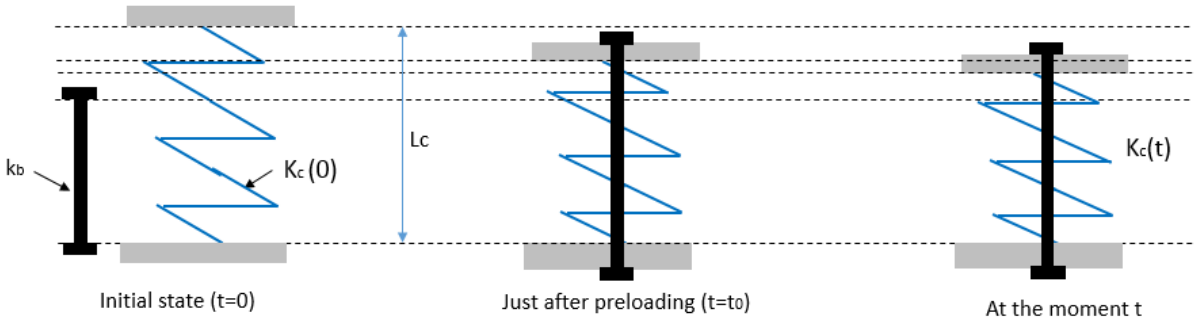


Fig.13. Deformation of the bolt and concrete due to creep and shrinkage

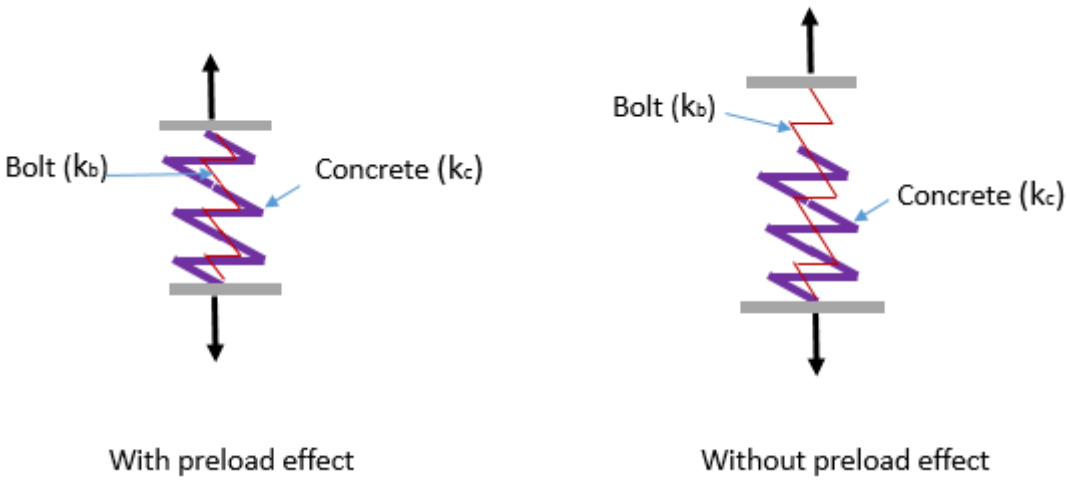


Fig.14. Bolt + concrete component

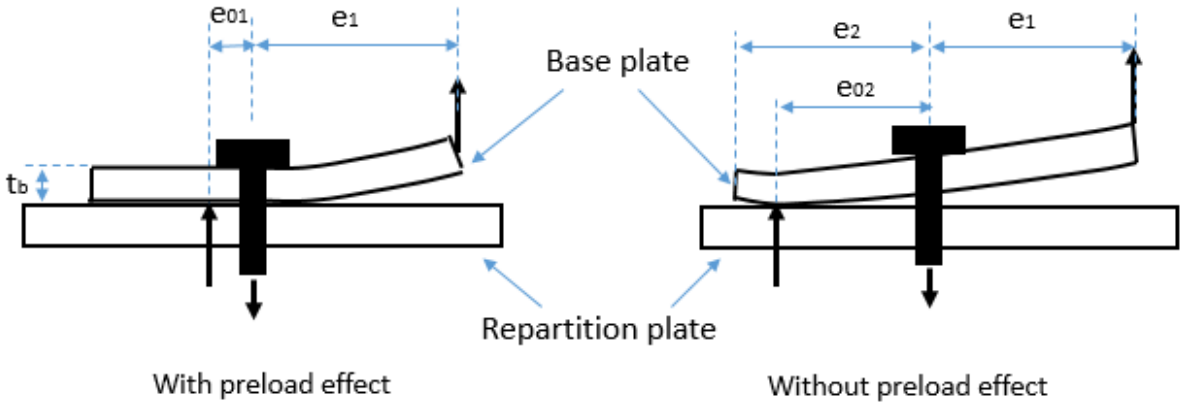


Fig.15. Position of the prying force

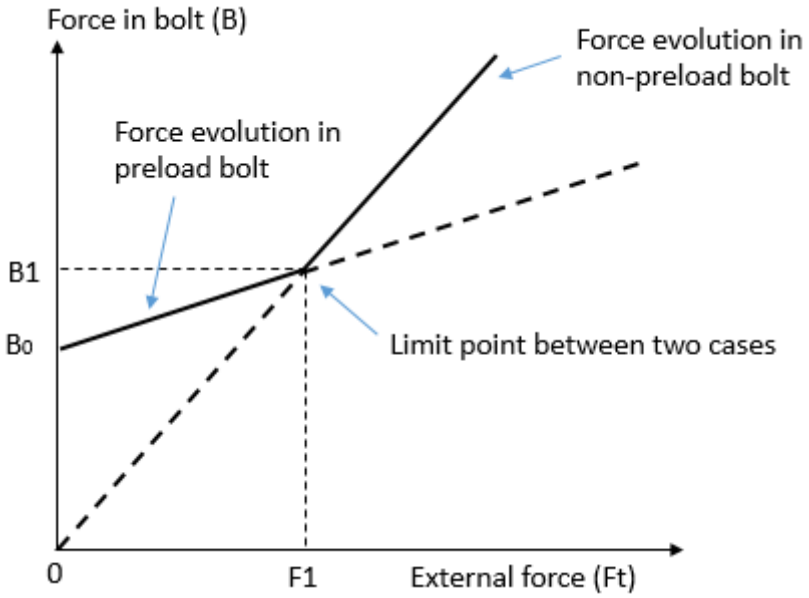


Fig.16. Evolution of the internal force in the bolts

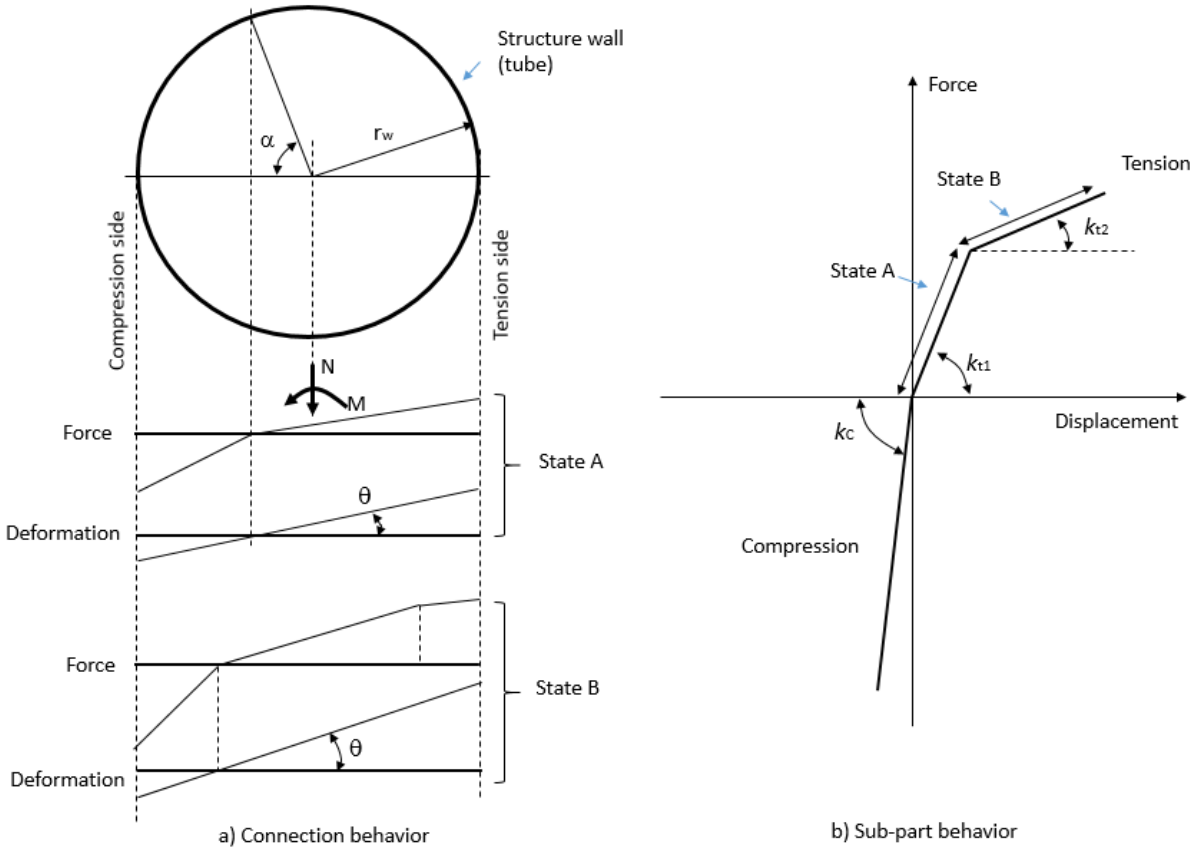


Fig.17. Behavior of the global connection

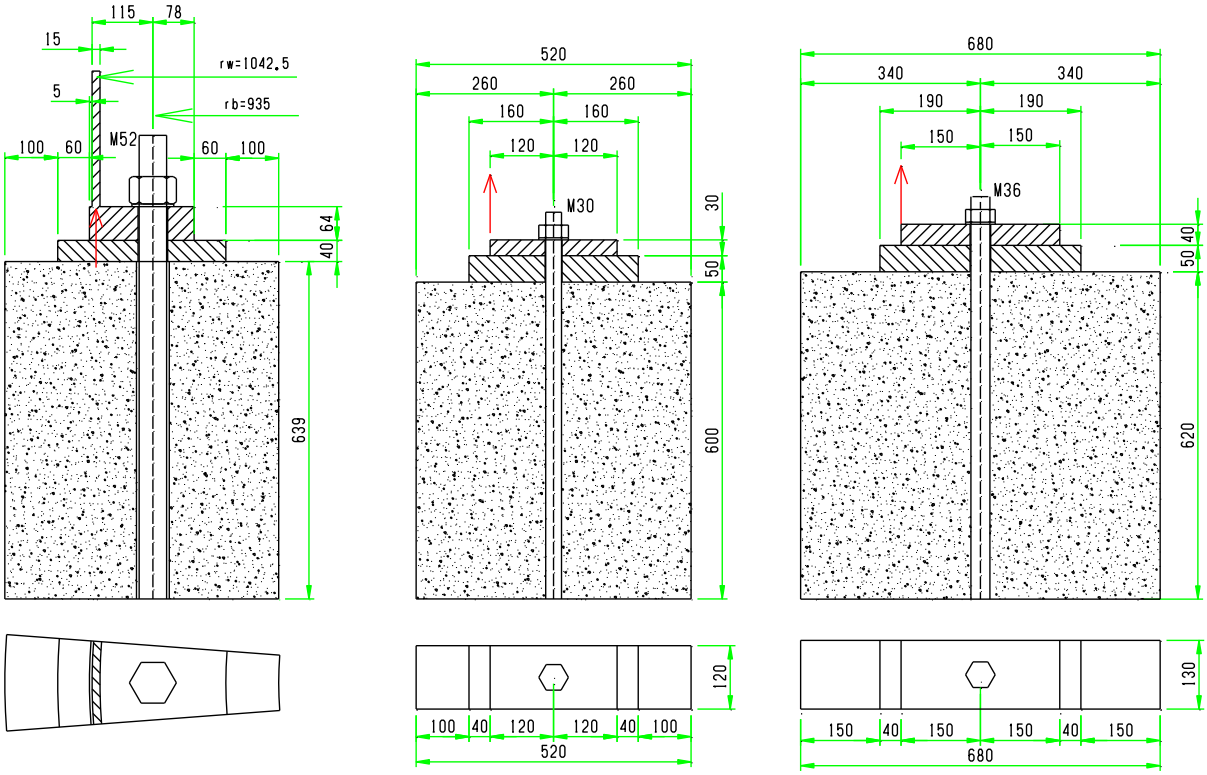


Ex 1.1- Ex 1.3 Ex 2.1 - Ex 2.2 Ex.3

Fig.18. Geometries of the numerical examples

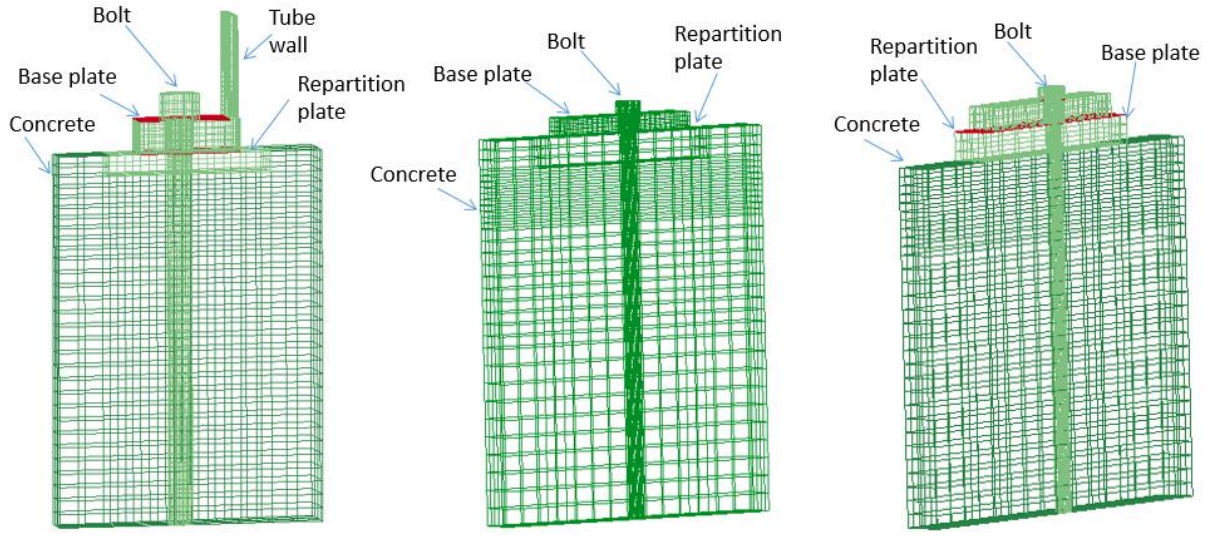


Ex 1.1 - Ex 1.3 Ex 2.1 - Ex 2.2 Ex.3

Fig.19. Used mesh for the examples

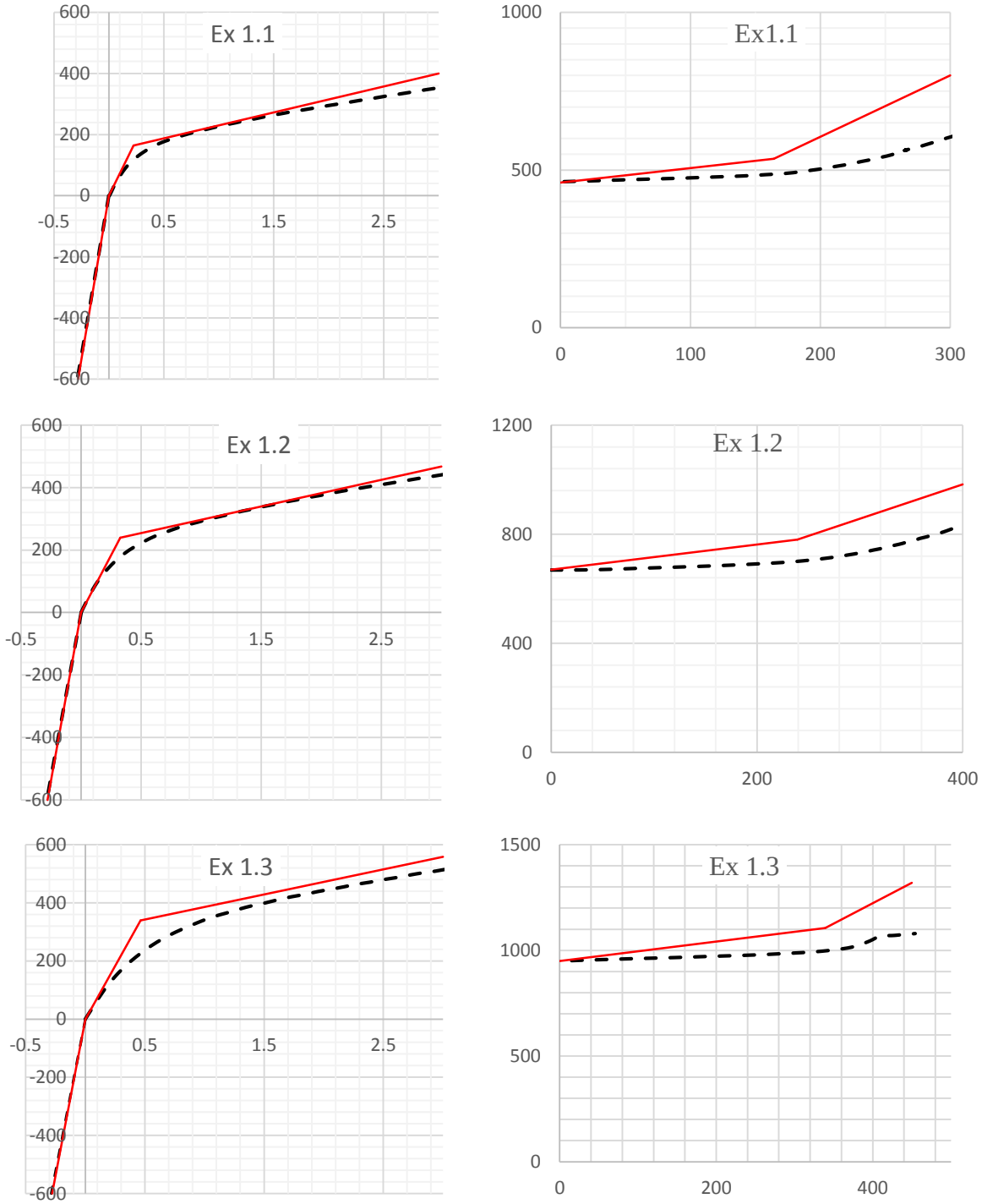


Load (vertical) - Displacement (horizontal) Bolt force (vetical) – Load (horizontal)

Analytical results are the continuous lines; Numerical results are the dashed lines; Units: kN, mm

Fig.20. Analytical vs. numerical results (Ex 1.1, 1.2 and 1.3)

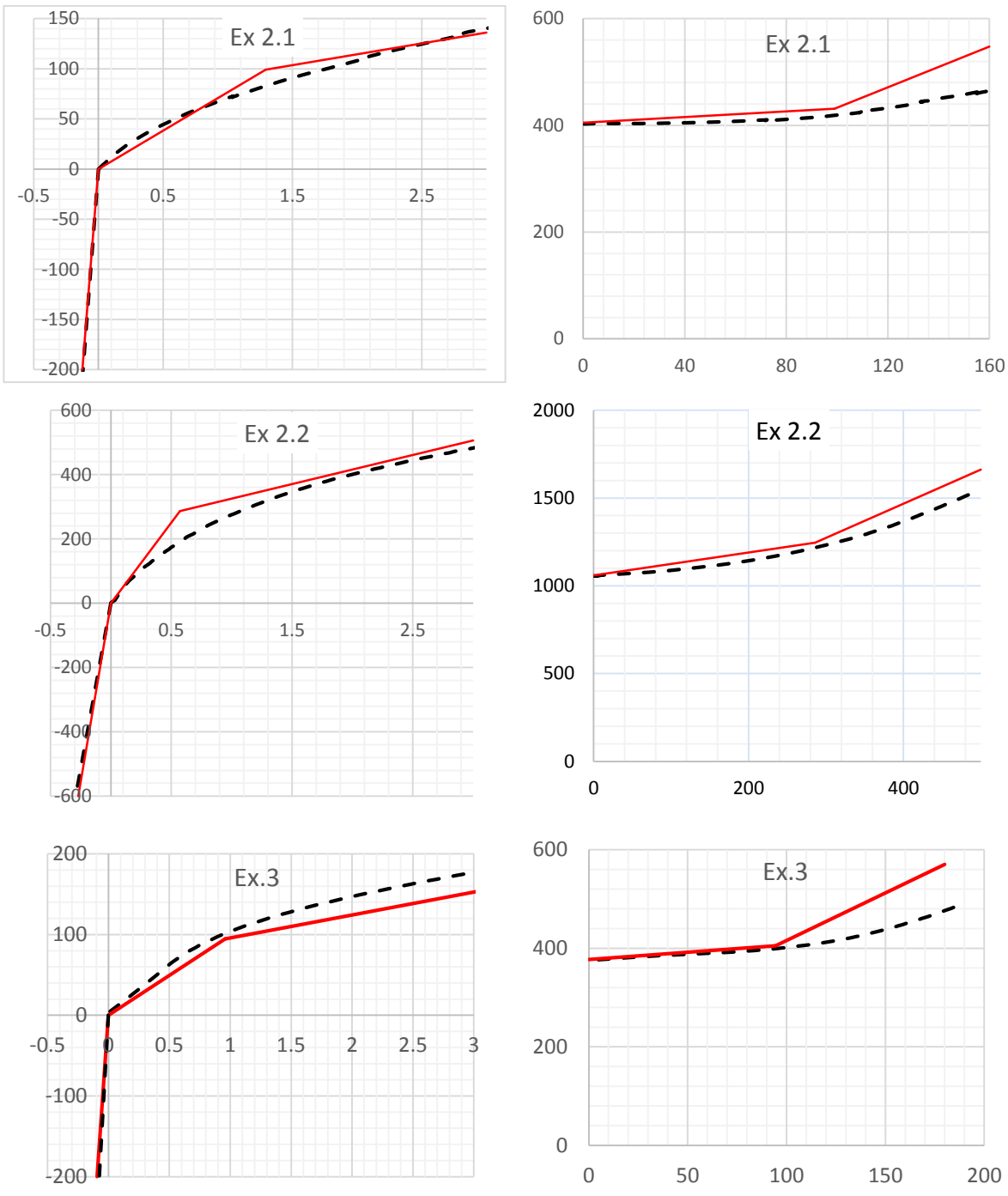


Load (vertical) - Displacement (horizontal)  Bolt force (vetical) – Load (horizontal)

Analytical results are the continuous lines; Numerical results are the dashed lines; Units: kN, mm

Fig.21. Analytical vs. numerical results (Ex 2.1 Ex 2.2 and Ex.3)

## List of Tables

Table 1: Stability function values

| $kl_b$ | 0 | 1 | 2 | 3 | 4 | 5 | 6 | 7 | 8 | 9 | 10 |
|---|---|---|---|---|---|---|---|---|---|---|---|
| $S$ | 4 | 4.13 | 4.51 | 5.08 | 5.80 | 6.61 | 7.48 | 8.39 | 9.33 | 10.29 | 11.25 |

Table 2: determination of $w_r$

| Cases | Formulas |
|---|---|
| Punctual contact (Figs. 9a and 9b) | |
| $c \le a_2$ | $w_r = 2c$ |
| $c > a_2$ | $w_r = 2a_2$ |
| Spread contact (Figs. 9c and 9d) | |
| $e_2 \ge t_b + d_w/2$ and $a_2 \ge c$ | $w_r = d_w + 2t_b + 2c$ |
| $e_2 < t_b + d_w/2$ and $a_2 \ge c$ | $w_r = 2e_2 + 2c$ |
| $e_2 \ge t_b + d_w/2$ and $a_2 < c$ | $w_r = d_w + 2t_b + 2a_2$ |
| $e_2 < t_b + d_w/2$ and $a_2 < c$ | $w_r = 2e_2 + 2a_2$ |

Table 3: Coefficient $\alpha_\Delta$

| $L_c/w_r$ | | **1.0** | **1.5** | **2.0** | **3.0** | **4.0** | **5.0** | **6.0** | **7.0** | **8.0** | **9.0** |
|---|---|---|---|---|---|---|---|---|---|---|---|
| $H_c/w_r$ | **1** | 0.95 | 0.72 | 0.66 | 0.63 | 0.63 | 0.63 | 0.63 | 0.63 | 0.63 | 0.63 |
| | **2** | 1.95 | 1.36 | 1.16 | 1.04 | 1.02 | 1.02 | 1.02 | 1.01 | 1.01 | 1.01 |
| | **3** | 2.93 | 2.00 | 1.65 | 1.36 | 1.28 | 1.25 | 1.25 | 1.25 | 1.25 | 1.24 |
| | **4** | 3.90 | 2.64 | 2.14 | 1.69 | 1.52 | 1.45 | 1.43 | 1.42 | 1.42 | 1.42 |
| | **5** | 4.88 | 3.28 | 2.63 | 2.02 | 1.76 | 1.64 | 1.59 | 1.56 | 1.55 | 1.55 |
| | **6** | 5.86 | 3.92 | 3.12 | 2.34 | 2.01 | 1.84 | 1.75 | 1.70 | 1.68 | 1.66 |
| | **7** | 6.84 | 4.56 | 3.61 | 2.66 | 2.25 | 2.04 | 1.91 | 1.84 | 1.80 | 1.77 |
| | **8** | 7.82 | 5.20 | 4.10 | 2.99 | 2.49 | 2.23 | 2.08 | 1.98 | 1.92 | 1.88 |

Table 4: Coefficient $\alpha_\theta$

| $L_c/w_r$ | 1.0 | 1.5 | 2.0 | 3.0 | $\ge 4.0$ |
|---|---|---|---|---|---|
| $\alpha_\theta$ | 5.95 | 4.46 | 4.18 | 4.03 | 3.89 |

Table 5: Analyse of the sub-part under tension with bolt preloading effect

*Mechanical model*

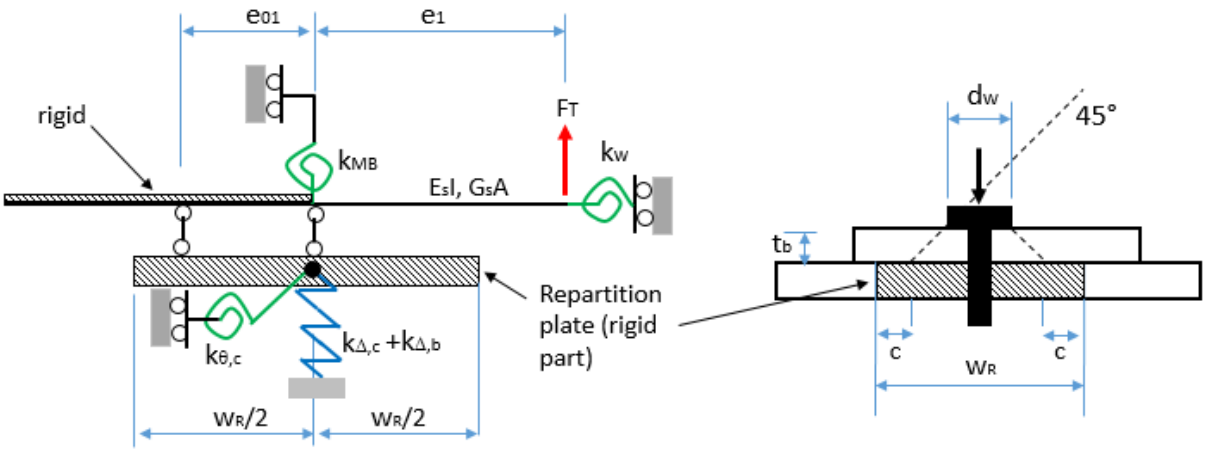


*Rigidity ($K_{t1}$):* $$K_{t1} = \left(\Omega_{FF} - \Omega_{1F}A_1 - \Omega_{2F}A_2\right)^{-1}$$

With: $$A_1 = \frac{\Omega_{2F}\Omega_{21} - \Omega_{1F}\Omega_{22}}{\Omega_{12}\Omega_{21} - \Omega_{11}\Omega_{22}},\ A_2 = \frac{\Omega_{1F}\Omega_{12} - \Omega_{2F}\Omega_{11}}{\Omega_{12}\Omega_{21} - \Omega_{11}\Omega_{22}}$$

$$\Omega_{11} = \frac{1}{k_{\theta,c}} + \frac{1}{k_{\theta,b}},\quad \Omega_{12} = \Omega_{21} = \frac{1}{k_{\theta,c}},\quad \Omega_{22} = \frac{e_1}{E_s I} + \frac{1}{k_{\theta,c}} + \frac{1}{k_w}$$

$$\Omega_{1F} = \frac{e_1}{k_{\theta,c}},\quad \Omega_{2F} = \frac{e_1^2}{2E_s I} + \frac{e_1}{k_{\theta,c}},\quad \Omega_{FF} = \frac{e_1^3}{3E_s I_1} + \frac{e_1}{G_s A} + \frac{e_1^2}{k_{\theta,c}} + \frac{1}{k_{\Delta,c}}$$

Axial force in the bolt: $$B = B_0 + F_T\left(\frac{e_1 + e_{01}}{e_{01}} - \frac{A_1 + A_2}{e_{01}}\right)\frac{k_{\Delta,b}}{k_{\Delta,b} + k_{\Delta,c}}$$

Maximal bending moment in the bolt: $M_b = F_T A_1$

Maximal stress in the bolt: $\sigma_b = B/A_b + M_b/W_b$

Bending moment in the tube wall: $M_w = F_T A_2$

*Limit point (Fig.16)*

$$B_1 = B_0\left(1 + \frac{k_{\Delta,b}}{k_{\Delta,c}}\right)$$

$$F_1 = B_0\left(1 + \frac{k_{\Delta,b}}{k_{\Delta,c}}\right)\left(\frac{e_1 + e_{01}}{e_{01}} - \frac{A_1 + A_2}{e_{01}}\right)^{-1}$$

*Remarks:*

$k_w$; $k_{\theta,b}$; $k_{\Delta,c}$ and $k_{\theta,c}$ are given in Eqs.(2), (5), (8) and (9) respectively.

$w_r$, is determined using Table 2.

Table 6: Analyse of the sub-part under tension without bolt preloading effect

*Mechanical model*

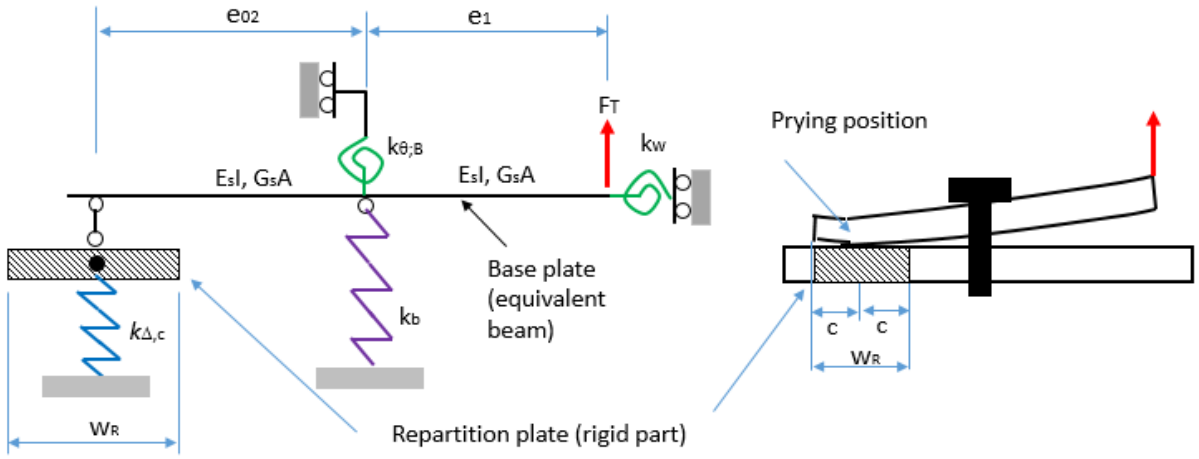


*Rigidity ($K_{t2}$)*

$$K_{t2} = \left(\Omega_{FF} - \Omega_{1F}A_1 - \Omega_{2F}A_2\right)^{-1}$$

With: $$A_1 = \frac{\Omega_{2F}\Omega_{21} - \Omega_{1F}\Omega_{22}}{\Omega_{12}\Omega_{21} - \Omega_{11}\Omega_{22}},\ A_2 = \frac{\Omega_{1F}\Omega_{12} - \Omega_{2F}\Omega_{11}}{\Omega_{12}\Omega_{21} - \Omega_{11}\Omega_{22}}$$

$$\Omega_{11} = \frac{e_{02}}{3E_sI} + \frac{1}{G_sAe_{02}} + \frac{1}{e_{02}^2k_{\Delta,b}} + \frac{1}{e_{02}^2k_{\Delta,c}} + \frac{1}{k_{\theta,\mathrm{b}}},\quad \Omega_{12} = \Omega_{21} = \frac{e_{02}}{3E_sI} + \frac{1}{G_sAe_{02}} + \frac{1}{e_{02}^2k_{\Delta,b}} + \frac{1}{e_{02}^2k_{\Delta,c}}$$

$$\Omega_{22} = \frac{1}{E_sI}\left(\frac{e_{02}}{3} + e_1\right) + \frac{1}{G_sAe_{02}} + \frac{1}{e_{02}^2k_{\Delta,b}} + \frac{1}{e_{02}^2k_{\Delta,c}} + \frac{1}{k_{\mathrm{w}}},\quad \Omega_{1F} = \frac{e_1e_{02}}{3E_sI} + \frac{e_1}{G_sAe_{02}} + \frac{e_1+e_{02}}{e_{02}^2k_{\Delta,b}} + \frac{e_1}{e_{02}^2k_{\Delta,c}}$$

$$\Omega_{2F} = \frac{1}{E_sI}\left(\frac{e_1e_{02}}{3} + \frac{e_1^2}{2}\right) + \frac{1}{G_sA}\frac{e_1}{e_{02}} + \frac{e_1+e_{02}}{e_{02}^2k_{\Delta,b}} + \frac{e_1}{e_0^2k_{\Delta,c}}$$

$$\Omega_{FF} = \frac{1}{E_sI}\left(\frac{e_1^2e_{02} + e_1^3}{3}\right) + \frac{1}{G_sA}\left(\frac{e_1^2}{e_{02}} + e_1\right) + \frac{(e_1+e_{02})^2}{e_{02}^2k_b} + \frac{e_1^2}{e_{02}^2k_{\Delta,c}}$$

Axial force in the bolt: $B = B_1 + (F_T - F_1)\left(\frac{e_1+e_{02}}{e_{02}} - \frac{A_1+A_2}{e_{02}}\right)$

Maximal bending moment in the bolt: $M_b = F_TA_1$

Maximal stress in the bolt: $\sigma_b = B/A_b + M_b/W_b$

Bending moment in the tube wall: $M_w = F_TA_2$

*Remarks:*

$k_{\mathrm{w}}$; $k_{\Delta,\mathrm{b}}$; $k_{\theta,\mathrm{b}}$ and $k_{\Delta,\mathrm{c}}$ are given in Eqs.(2), (4), (5) and (8) respectively

$F_1$ is given in Table 5.

$w_{\mathrm{r}}$ is determined using Table 2.

Table 7: Analyse of the sub-part under compression

*Mechanical model*

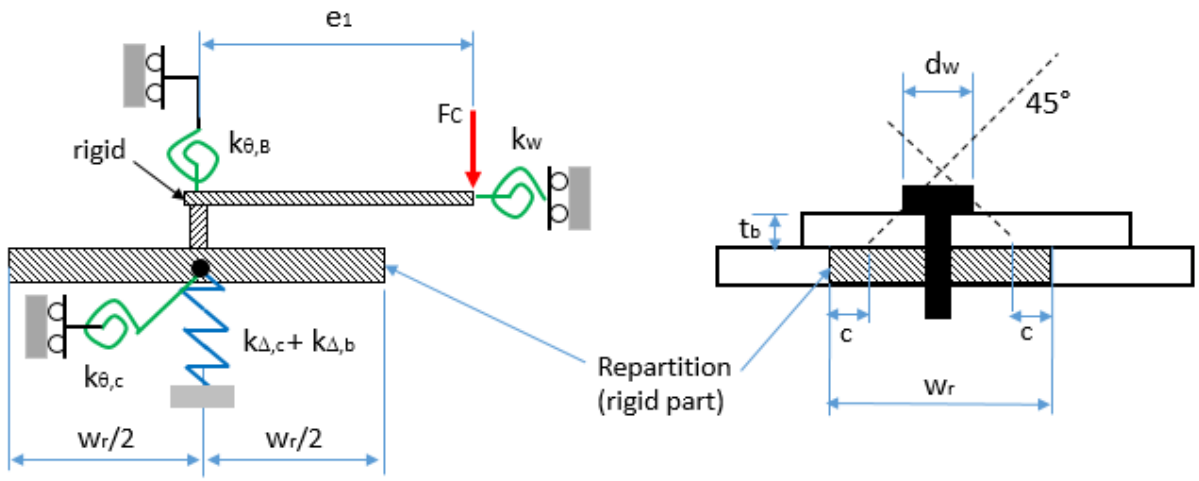


*Rigidity ($K_c$):*

$$K_c = \left(\Omega_{FF} - \Omega_{1F} A_1 - \Omega_{2F} A_2\right)^{-1}$$

With:

$$A_1 = \frac{\Omega_{2F}\Omega_{21} - \Omega_{1F}\Omega_{22}}{\Omega_{12}\Omega_{21} - \Omega_{11}\Omega_{22}},\ A_2 = \frac{\Omega_{1F}\Omega_{12} - \Omega_{2F}\Omega_{11}}{\Omega_{12}\Omega_{21} - \Omega_{11}\Omega_{22}}$$

$$\Omega_{11} = \frac{1}{k_{\theta,c}} + \frac{1}{k_{\theta,\mathrm{b}}},\quad \Omega_{12} = \Omega_{21} = \frac{1}{k_{\theta,c}},\quad \Omega_{22} = \frac{1}{k_{\theta,c}} + \frac{1}{k_{\mathrm{w}}}$$

$$\Omega_{1F} = \frac{e_1}{k_{\theta,c}},\quad \Omega_{2F} = \frac{e_1}{k_{\theta,c}},\quad \Omega_{FF} = \frac{1}{k_{\Delta,c} + k_{\Delta,b}} + \frac{e_1^2}{k_{\theta,c}}$$

*Remarks:*

$k_{\mathrm{w}}$; $k_{\Delta,\mathrm{b}}$; $k_{\theta,\mathrm{b}}$; $k_{\Delta,\mathrm{c}}$ and $k_{\theta,\mathrm{c}}$ are given in Eqs.(2), (4), (5), (8) and (9) respectively

$w_{\mathrm{r}}$, is determined using Table 2.

Table 8: input data and results given by the analytical method

| Quantities | | | Examples | | | | | | | | | | | | | | | |
|---|---|---|---|---|---|---|---|---|---|---|---|---|---|---|---|---|---|---|
| Symbol | Reference | Unit | Ex.1.1 | | | Ex.1.2 | | | Ex.1.3 | | | Ex.2.1 | | | Ex.2.2 | | | |
| | | | (1) (*) | (2) (*) | (3) (*) | (1) (*) | (2) (*) | (3) (*) | (1) (*) | (2) (*) | (3) (*) | (1) (*) | (2) (*) | (3) (*) | (1) (*) | (2) (*) | (3) (*) | |
| Material, geometries and preloading (the same geometry (Fig.1) for Ex. 1.1 , Ex.1.2 and Ex.1.3; the same geometry (Fig.1) for Ex.2.1 and Ex.2.2) | | | | | | | | | | | | | | | | | | |
| $E$ | Young modulus | kN/mm$^2$ | 210.0 | | | | | | | | | 210.0 | | | 1680.0 | | | |
| $E_b$ | | kN/mm$^2$ | 210.0 | | | | | | | | | 210.0 | | | 630.0 | | | |
| $E_c$ | | kN/mm$^2$ | 31.0 | | | | | | | | | 31.0 | | | 31.0 | | | |
| $r_b$ | Geometries (Figs.1 & 18) | mm | 935 | | | | | | | | | - | | | | | | |
| $b^{(**)}$ | | mm | 140.6 | | | | | | | | | 120.0 | | | | | | |
| $t_b$ | | mm | 64.0 | | | | | | | | | 30.0 | | | | | | |
| $t_p$ | | mm | 40.0 | | | | | | | | | 50.0 | | | | | | |
| $t_w$ | | mm | 15.0 | | | | | | | | | - | | | | | | |
| $r_w$ | | mm | 1042.5 | | | | | | | | | - | | | | | | |
| $l_b$ | | mm | 743.0 | | | | | | | | | 680.0 | | | | | | |
| $d$ | | mm | 46.5 | | | | | | | | | 27.0 | | | | | | |
| $d_w$ | | mm | 78.0 | | | | | | | | | 56.0 | | | | | | |
| $H_c$ | | mm | 639.0 | | | | | | | | | 600.0 | | | | | | |
| $e_1$ | | mm | 107.5 | | | | | | | | | 12.0 | | | | | | |
| $e_2$ | | mm | 78.0 | | | | | | | | | 12.0 | | | | | | |
| $B_0$ | Preloading | kN | 460.0 | 460.0 | 460.0 | 670.0 | 670.0 | 670.0 | 950.0 | 950.0 | 950.0 | 405.0 | 405.0 | 405.0 | 1060.0 | 1060.0 | 1060.0 | |
| Intermediate quantities | | | | | | | | | | | | | | | | | | |
| $e_{01}$ | Eq.(13) | mm | 47.36 | - | - | 47.36 | - | - | 47.36 | - | - | 35.7 | - | - | 35.7 | - | - | |
| $e_{02}$ | Eq.(14) | | - | 78 | - | - | 78 | - | - | 78 | - | - | 120 | - | - | 120 | - | |
| $b_{eff}$ | Eq.(3) | mm | 119.51 | 119.51 | 119.51 | 119.51 | 119.51 | 119.51 | 119.51 | 119.51 | 119.51 | 102 | 102 | 102 | 102 | 102 | 102 | |
| $w_r$ | Table 2 | mm | 256 | 10 | 256 | 256 | 10 | 256 | 256 | 10 | 256 | 241 | 80 | 241 | 320 | 80 | 320 | |
| $L_c$ | (***) | mm | 476 | 320 | 476 | 476 | 320 | 476 | 476 | 320 | 476 | 520 | 280 | 520 | 520 | 280 | 520 | |
| $\alpha_\Delta$ | Table 3 | - | 1.49 | 2.46 | 1.49 | 1.49 | 2.46 | 1.49 | 1.49 | 2.46 | 1.49 | 1.37 | 2.60 | 1.37 | 1.23 | 2.60 | 1.23 | |
| $\alpha_\theta$ | Table 4 | - | 4.27 | - | 4.27 | 4.27 | - | 4.27 | 4.27 | - | 4.27 | 4.15 | - | 4.15 | 4.39 | - | 4.39 | |
| $e_1$ | Figs. 1 & 18 | mm | - | - | 107.5 | - | - | 107.5 | - | - | 107.5 | - | - | 120 | - | - | 120 | |
| $e_x$ | Fig.18 | mm | - | - | 12.5 | - | - | 12.5 | - | - | 12.5 | - | - | 0.00 | - | - | 0.00 | |
| $S$ | Eq.(6) | - | 4.66 | 4.66 | 4.66 | 4.93 | 4.93 | 4.93 | 5.28 | 5.28 | 5.28 | 7.35 | 7.35 | 7.35 | 7.00 | 7.00 | 7.00 | |
| $k_w$ | Eq.(2) | kNm | 18.76 | 18.76 | 18.76 | 18.76 | 18.76 | 18.76 | 18.76 | 18.76 | 18.76 | - | - | - | - | - | - | |
| $k_{\Delta,b}$ | Eq.(4) | kN/mm | 479.74 | 479.74 | 479.74 | 479.74 | 479.74 | 479.74 | 479.74 | 479.74 | 479.74 | 176.73 | 176.73 | 176.73 | 530.19 | 530.19 | 530.19 | |
| $k_{\theta,b}$ | Eq.(5) | kNm | 30.21 | 30.21 | 30.21 | 32.00 | 32.00 | 32.00 | 34.25 | 34.25 | 34.25 | 5.92 | 5.92 | 5.92 | 16.93 | 16.93 | 16.93 | |
| $k_{\Delta,c}$ | Eq.(8) | kN/mm | 2925.2 | 1771.8 | 2925.2 | 2925.2 | 1771.8 | 2925.2 | 2925.2 | 1771.8 | 2925.2 | 2715.3 | 1430.8 | 2715.3 | 3017.0 | 1430.8 | 3017.0 | |
| $k_{\theta,c}$ | Eq.(9) | kNm | 6689.6 | - | 6689.6 | 6689.6 | - | 6689.6 | 6689.6 | - | 6689.6 | 5206.3 | - | 5206.0 | 8677.2 | - | 8673.2 | |
| Final results (the global rigidities ($K_t$ or $K_c$), point ($B_1$, $F_1$) from which the effect of the preloading is considered as absence (Fig. 16)) | | | | | | | | | | | | | | | | | | |
| $K_t$ ($K_c$) | Tables 5-7 | kN/mm | 730.79 | 84.95 | 2150.2 | 730.81 | 85.48 | 2149.9 | 730.84 | 86.15 | 2150.2 | 76.58 | 21.77 | 1607.6 | 499.46 | 90.58 | 2233.7 | |
| $B_1$ | Table 5 | kN | 535.44 | - | - | 779.88 | - | - | 1105.8 | - | - | 431.36 | - | - | 1246.3 | - | - | |
| $F_1$ | Table 5 | kN | 164.25 | - | - | 239.28 | - | - | 339.36 | - | - | 98.99 | - | - | 286.18 | - | - | |

(*): (1) = in tension with preloading; (2) = in tension without preloading; and (3) = in compression (always with preloading)
(**): for Ex 1.1, 1.2 and 1.3, b is calculated using Eq.(1), while b is obtained using Fig.18. for Ex 2.1., 2.2.
(***): $L_c$ is determined from the dimension of the rigid part of the repartition plate ($w_r$) and from the actual geometries of the concrete block (Fig.18) such that $L_c$ is symmetric with respect to $w_r$.